Microchimica Acta (2022) 189: 190
https://doi.org/10.1007/s00604-022-05259-9

REVIEW ARTICLE

An insight into the potentials of carbon dots for in vitro live-cell imaging: recent progress, challenges, and prospects

Zahra Hallaji[1] · Zeinab Bagheri[2] · Mahdi Oroujlo[2] · Mehrnoosh Nemati[2] · Zeinab Tavassoli[3] · Bijan Ranjbar[1,4]

Received: 8 December 2021 / Accepted: 3 March 2022 / Published online: 13 April 2022

Abstract

Carbon dots (CDs) are a strong alternative to conventional fluorescent probes for cell imaging due to their brightness, photostability, tunable fluorescence emission, low toxicity, inexpensive preparation, and chemical diversity. Improving the targeting efficiency by modulation of the surface functional groups and understanding the mechanisms of targeted imaging are the most challenging issues in cell imaging by CDs. Firstly, we briefly discuss important features of fluorescent CDs for live-cell imaging application in this review. Then, the newest modulated CDs for targeted live-cell imaging of whole-cell, cell organelles, pH, ions, small molecules, and proteins are elaborately discussed, and their challenges in these fields are explained.

Keywords Carbon dots · Fluorescence · Live-cell imaging · In vitro · Targeting

Introduction

In vitro live-cell imaging is the study of the cellular structure and function in living cells, requiring advanced technologies to record the high-resolution and spatiotemporal images of cellular events such as migration, cellular development, and intracellular trafficking. The progress of this field depends on the efforts to synthesize new fluorescent reagents, develop new microscopy techniques, and finally increase the understanding of the complex nature of cellular structures and functions [1, 2]. Fluorescent reagents used in live-cell imaging need to have specialized optical, chemical, and biological properties, such as brightness, photostability, fluorogenicity, biocompatibility, chemical stability, and up-conversion. The fluorescent probes used commonly in live-cell imaging are composed of organic dyes, quantum dots (QDs), fluorescent proteins, and CDs [3–7].

Currently, great progress has been made in the development of green fluorescent proteins, but the development of other colors of fluorescent proteins is in the early stages [8–14]. In addition, their short fluorescence lifetime and high requirements of the operation process are factors that limit their development [6]. Organic dyes are the most common markers that show high brightness in biological environments and undergo an appropriate number of switching cycles, but the photobleaching and the buffer-dependent blinking limit their applications [15–23]. QDs as a new nano-size material represents attractive optical properties, including very low photobleaching, high absorption coefficient, and remarkable brightness, but the defect of fast blinking is not resolved yet in these nano-particles. Additionally, high on–off duty cycle and high toxicity have reduced the QD applications [24–28].

CDs are carbon-based structures and belong to the fluorescent emissive nano-materials [29]. They have applied in various new technologies and medical science such as optical devices, sensors, catalysis, drug delivery, and bioimaging [30]. These nano-particles have zero-dimensional size (typically ~5 nm), unique multicolor emission, appropriate solubility, and low toxicity, but their brilliant properties are simple and low-cost synthesis procedures. Another exciting feature of CDs is their graphitic-like core structure with the

✉ Zeinab Bagheri
ze_bagheri@sbu.ac.ir

✉ Bijan Ranjbar
ranjbarb@modares.ac.ir

1 Department of Nanobiotechnology, Faculty of Biological Sciences, Tarbiat Modares University, 14117-13116 Tehran, Iran

2 Faculty of Life Sciences and Biotechnology, Shahid Beheshti University, 1983963113 Tehran, Iran

3 Department of Biology, Islamic Azad University Central Tehran Branch, Tehran, Iran

4 Department of Biophysics, Faculty of Biological Sciences, Tarbiat Modares University, 14117-13116 Tehran, Iran

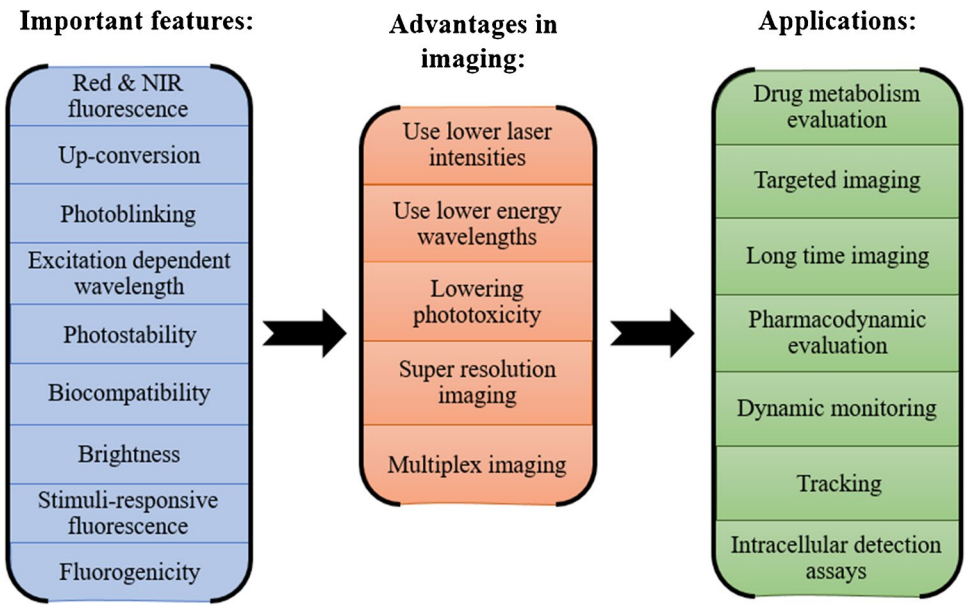

Scheme 1 Important features, advantages, and applications of CDs in live-cell imaging

possibility of bonding to the various chemical groups, while nitrogen, sulfur, and phosphorus doping into its structure make them more attractive [31–36]. CDs are easily obtained from simple reactants and expose remarkable photostability [37, 38]. CDs can emit durable multicolor fluorescence light [39, 40] and enable the imaging of live cells via their photostability and biocompatibility [41, 42]. This nano-particle easily interacts with the cellular membranes and penetrates to the cytoplasm via the endocytosis process [43]. Dependence of fluorescence emission to the excitation wavelength is responsible for multicolor imaging of cells or organelles by the CDs [44, 45]. Furthermore, the pH of the cellular environment can affect the fluorescent emission of CDs that provide the advantage of cell pH detection by these nanoparticles [46]. Hydrophilicity, chemical functional groups, and the electrical charges of the CD surface are key factors in their penetration into the cells and targeting of organelles [45–48]. All of these properties can be modulated rationally during the synthesis process and post modification of CDs [36, 49].

All these features have led the CDs to various fluorescence imaging applications. The aspects of this topic and the obtained results have been compiled and categorized in some review articles during the last years, covering the common uses of CDs in fluorescence in vivo imaging, high-resolution imaging, and intercellular organelle targeting [3, 50–58]. Meanwhile, the importance of in vitro live-cell imaging technologies in pharmaceuticals and the necessity of the continuous introduction of the new nano-based probes with various critical characteristics are still attractive and challenging issues in this area. Hence, this review has focused on these new possibilities and provides the latest progress in live-cell imaging using novel modulated CDs. To the best of the authors' knowledge, no review article has been published on this topic. A list of the CD advantages and their applications in live-cell imagining are presented in Scheme 1.

CD properties for in vitro live-cell imaging

The properties of CDs vary according to the precursors and the synthesis method, which is very explained in various review articles [51, 57–65]. Thus, among the features of CDs, only important features related to in vitro live-cell imaging are briefly summarized in this section.

Red and near infrared (NIR) fluorescence

The CD fluorescent emission wavelength has a broad range from deep UV to NIR region [41, 42], with large Stokes shifts originating from the different electronic transition pathways [42]. NIR fluorescence emission is generally generated by the large rigid conjugated structure of CDs and their quantum confinement effect. In this range, due to the reduction of tissue absorption and inherent fluorescence of the biological environment, the depth of light penetration is greater. Therefore, extensive research has recently been conducted on the synthesis and preparation of long-wavelength CDs that have lowered phototoxicity in the biological transparency window [36]. For example, D-π-A-conjugated fluorine and nitrogen-doped CDs were prepared from uric acid and NH_4F as doping agents via the solvothermal method. Because of the D-π-A-conjugated formation, prepared CDs show absorption peaks in the full UV–Vis–NIR spectrum. In addition to the excellent cytocompatibility and appropriate

cellular uptake, the brilliant property of these CDs is their very sharp deep-red emission that confirms their competence for cell imaging applications (Fig. 1A) [66].

Up-conversion fluorescence

Up-conversion fluorescence is often cited as an important feature in CDs. It can be detected by measuring the excitation intensity dependence of the fluorescence [67]. Multiphoton excitation provides the capability of deep-tissue penetration by using lower energy wavelength during the bioimaging process. Recently, a new class of CDs was obtained using p-aminoazobenzene as a nitrogen doping precursor with remarkable properties, including high affinity to the RNA, red fluorescence emission, two-photon excitation, and photodynamic activity. Owing to these characteristics, CDs enable real-time fluorescence monitoring of dynamic nucleolar changes during photodynamic therapy. Because of the overlapping between CD and RNA adsorption, a two-photon laser was used to stimulate CD at 700 nm ($\lambda_{em} = 625$) to prevent adsorption overlap (Fig. 1B) [68].

Multicolor imaging

In contrast with organic dyes and inorganic QDs, the emission peak of some CDs exhibits excitation-dependent behavior. In other words, the emission wavelength of CDs changes in the different excitation wavelengths that are considerable for multicolor and high-resolution imaging applications [69, 70]. This phenomenon is related to the changes in the size distribution and the number of surface defects in the CDs [71]. According to a novel report, in vitro imaging of human umbilical vein endothelial cells were done by the VEGF-conjugated CDs. The CDs were firstly obtained via the hydrothermal method and then conjugated with VEGF by carbodiimide coupling. As shown in Fig. 1C, multicolor emission was observed due to the excitation wavelength-dependent emission of CDs [72].

Photostability

Photobleaching is the biggest problem of fluorescent dyes that strongly restricts their imaging efficiency [73]. In addition, photobleaching makes storing and preparing samples difficult because it also occurs under natural light irradiation. By resistance to the photobleaching, the CDs provide longer imaging time and overcome all mentioned limitations [74]. For example, the green synthesis of CDs was prepared by using sugarcane as the sole carbon precursor. Based on this study, doping of nitrogen and phosphorus is responsible for better solubility, high quantum yield (QY), and photostability of synthesized CDs. In order to investigate the possibility of photobleaching CDs, the effect of continuous ultraviolet light was studied using a 365-nm lamp for 2 h. As shown in Fig. 1D, CDs display only 23% decay [75].

Photoblinking

Spontaneous photoblinking is the other attractive feature of some CDs that is necessary for super-resolution imaging. Usually, to prevent emission overlapping from neighboring fluorophores, a small section of the sample is isolated and selected for the imaging process. Therefore, a kind of photoswitchable fluorescent probes or devices such as interference grids is required for this purpose. Interference grid role is to excite a select population of fluorophores at the same time within one sample. Some modulated CDs are capable of switching from an "on" emission state to an "off" state under continuous illumination, so there is no need for additional adjustment [76]. Malic acid-CDs are a clear example of a photoswitchable probe that exhibited an acceptable signal-to-noise ratio in different imaging buffer solutions. Because of their photoblinking properties, this kind of CD is able to significantly enhance spatial resolution in imaging experiments. Figure 1E shows the bright spots of malic acid-CDs in the on-state were distributed throughout the imaging session [42].

Brightness

The fluorescence output per fluorophore molecule, known as brightness, is proportional to the extinction coefficient and the fluorescence QY. Lower laser intensity is needed to excite fluorophores with higher brightness, providing higher resolution imaging and lower phototoxicity for live cells. Many different approaches exist to enhance the brightness of semiconductor QDs or metal nano-particles, but controlling CD synthesis in order to achieve more brightness is significantly easy and more accessible. For example, a simple one-step approach was utilized to prepare bright multicolor CDs with QY up to 58%. These CDs were used for bioimaging of HeLa cell that showed bright confocal images (Fig. 1F). Also, CDs show a high dopamine neurotransmitter fluorometric detection ability in the blood plasma samples without any surface functionalization [77].

Stimulus-responsive fluorescence

CDs are able to change their optical properties in response to stimuli such as pH, light radiation, and analytes (gases, ions, biologically active molecules, etc.). By responding to stimuli, such materials have been used as Forster resonance energy transfer (FRET) fluorophores. The ratiometric fluorescence sensing in FRET requires two or more fluorophores with different emission bands: one of them is a reference, and others act as a response molecule [78]. By considering

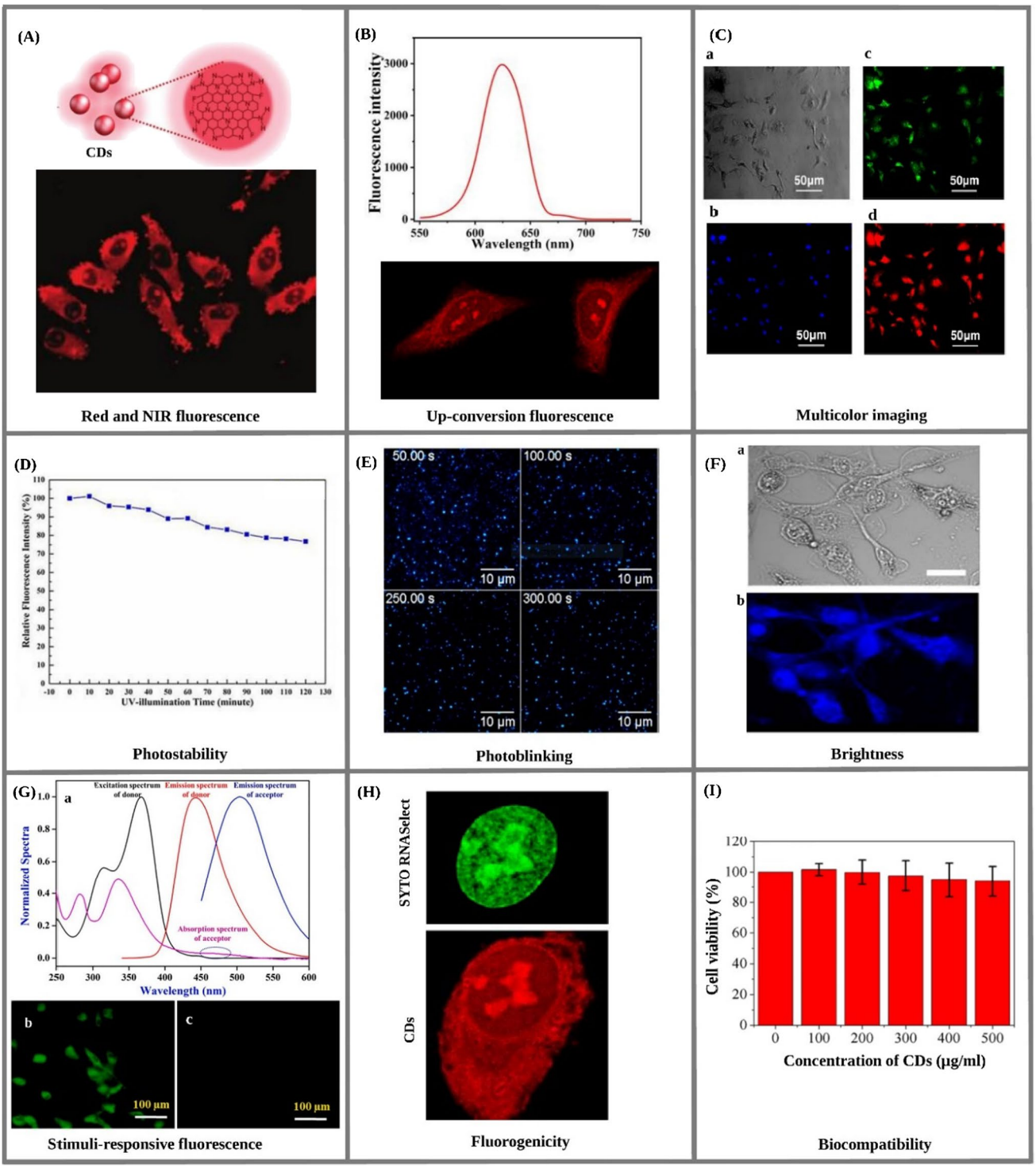

CD advantages in comparison with common fluorophores, CD-based FRET systems are introduced to the biosensing and bioimaging application. A recent examination has used the pyrolysis method to prepare CDs from porcine pancreatic lipase (PPL). The synthesized CDs are used as a fluorescence probe for the detection of dopamine. The tendency to oxidization into the dopamine-quinone triggered the adsorption of dopamine on the CD surface and effectively quenched the CD emission. As shown in Fig. 1G(a), the absorption spectrum of dopamine-quinone has an overlap with the emission spectrum of CDs, and this overlapping shows the occurrence of FRET. As a result, quenching of CD fluorescent emission is a sensitive sensing way of dopamine detection (Fig. 1G(b, c)) [79].

◂**Fig. 1** **A** Confocal laser scanning microscopy (CLSM) images of HepG2 cells treated with CDs, Reproduced with permission from ref [66]. Copyright 2020 Wiley–VCH. (**B**) The emission spectrum of prepared CDs excited by a 700-nm two-photon laser and two-photon image of HeLa cells incubated with CDs. Reproduced with permission from ref [68]. Copyright 2021 Elsevier. (**C**) CLSM images of HUVEC cells incubated with CDs taken at different excitation wavelengths: (a) bright field, (b) 403, (c) 488, and (d) 640 nm. Reproduced with permission from ref [72]. Copyright 2020 American Chemical Society. (**D**) CDs show only 23% decay in the period of 2 h at 365-nm irradiation [75]. (**E**) On–off fluorescence imaging of CDs. Reproduced with permission from ref [42]. Copyright 2018 American Chemical Society. (**F**) CLSM of PC-12 cells treated with CDs: (a) bright-field image and (b) confocal images taken by excited at 401. Reproduced with permission from ref [77]. Copyright 2017 American Chemical Society. (**G**) (a) Spectral overlap between the fluorescence spectrum of CDs and the absorption spectrum of dopamine-quinone during the FRET process, the image of MDA-MB 468 cells incubated with (b) the 10 μg/mL of CDs, and (c) after adding dopamine solution at the excitation wavelength (450–480 nm). Reproduced with permission from ref [79]. Copyright 2020 Elsevier. (**H**) Comparative staining with CDs and SYTO RNASelect. Reproduced with permission from ref [81]. Copyright 2019 American Chemical Society. (**I**) The cytotoxic effects of CDs against HeLa cells with 94% cell viability even at 500 μg/mL. Reproduced with permission from ref [87]. Copyright 2020 American Chemical Society

Fluorogenicity

Fluorogenicity explains the enhancement of a fluorophore emission during the interaction with its target molecule. This dramatically removes background fluorescence from the unspecific localization of probes in live cells and other biological environments [80]. For example, CDs exhibit fluorescence emission, which is able to photostable, wash-free, high-resolution, and high-quality nucleolar imaging. Most RNAs accumulate in the nucleoli that could be stained clearly by CDs. With a high affinity to the nucleolus and excellent imaging performance, CDs have exposed more advantages to the commercial nucleolar dye (Fig. 1H) [81].

Biocompatibility

Carbon is the basic element of life and constitutes the body of living organisms. Therefore, carbon-based nano-materials such as CDs are biocompatible with living organisms and different cell lines [42, 82–85]. In vivo examination confirms the nontoxic nature of CDs in zebrafish as an animal model [86]. Water-soluble fluorescent-nitrogen-doped CDs were synthesized from the lemon juice and ethylenediamine via hydrothermal methods. The fluorescence emission intensity of reported CDs depends on the pH value and shows appropriate photostability under different salt conditions. Biocompatibility and nontoxicity of these CDs were demonstrated by the 3-(4,5-dimethylthiazol-2-yl)-2,5-diphenyltetrazolium bromide (MTT) assay of the MCF7 cell lines (Fig. 1I) [87].

Applications of CDs for in vitro live-cell imaging

The obvious understanding and tracking of biochemical and physiological streams in all biological levels (biomacromolecules, cellular level, tissues, and body organs) are easily and quickly available via various cell imaging methods. The existing organic dyes and semiconductor QDs are challenged with related photobleaching, poor water solubility, and intrinsic toxicity. Due to their stable photoluminescence, multicolor emission, low cytotoxicity, and good biocompatibility, CDs are a powerful alternative for common bioimaging dyes. In the following, the last advances in CD-based in vitro live-cell imaging, including whole cell, cell organelles, pH, ion, molecule, and protein imaging, are discussed in detail (Scheme 2).

Whole-cell imaging (cytoplasm imaging)

A wide variety of CDs with different optical properties are applied to cell imaging without any requirement for external transfection and specific ligand [75, 88–92]. The penetration mechanism of CDs into the cells are mainly consists of endocytosis, aquaporins aided entrance, and diffusion through the ion channels [93].

In an advanced report, *Citrus limon* was selected as a low-cost carbon source for synthesizing nitrogen-doped CDs via a hydrothermal approach. The MCF7 cells are treated with 0.025 mg/mL of obtained CDs to examine their bioimaging potency. All blue, green, and red colors luminescence are recorded separately in the cytoplasm region, revealing sufficient CD entrance to the sample cells. The brightness of stained cells with reported CDs proved their competence as a multicolor probe for whole-cell imaging [89]. Other high biocompatible nitrogen-doped CDs were prepared by the hydrothermal procedure. Figure 2 shows the blue, green, and red fluorescence images of the HeLa cells after incubation with 100 μg mL^{-1} of CDs under different times and excitation wavelengths. Increasing the incubation time provides more opportunities for accumulation of the CDs into the cytoplasm and causes higher fluorescent emission. This indicates the appropriate permeability of CDs across the HeLa membrane cells [87]. Nitrogen and sulfur-doped CDs were synthesized from scallion and applied as imaging agents of the A549 cells. After incubation in prepared CDs, the A549 cells were excited at 405 nm by fluorescence microscopy. According to the observation of the resulting images, the main fluorescent light comes from perinuclear regions of the cytosol. As a result, surface functional groups and the small size of reported CDs are responsible for their excellent cell permeability into the living cells [91].

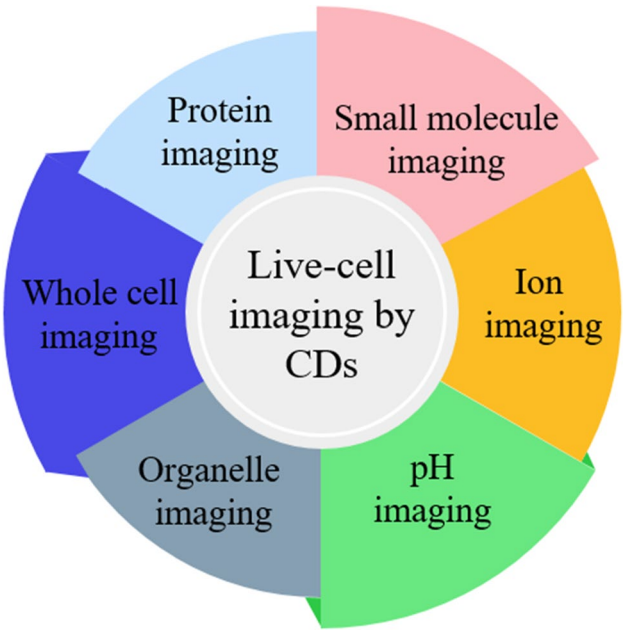

Scheme 2 Application potential of fluorescent CDs as a live-cell imaging probe

Because of sufficient penetration and accumulation into various cells, the emission light of CDs is appropriately detected and pictured by fluorescent microscopy. One of the entrance ways is related to the basic molecule derivatives such as arginine. The guanidyl group in arginine has a positive charge, which can electrostatically bind with the negative components of the plasma membrane and trigger the endocytosis process [94]. In spite of some reports, there is no strong explanation about the exact mechanism of CD uptake by the cells.

Organelle imaging

The mechanism of diseases, growth, repair, and many other molecular pathways is detectable and understandable via subcellular imaging. A wide variety of organelles are targeted in this imaging field, including lysosome, nucleus, nucleolus, mitochondria, endoplasmic reticulum (ER), and lipid droplet. The main difficulties of organelles imaging are the entrance of the probe into the cell and its specific attachment to the target. Typically, the colocalization experiment with proven commercial probes such as LysoTracker Deep Red and NucRed Live 647 is performed to track the precise probe location. The common targets of subcellular imaging by using CDs are presented in the following.

Lysosome

The lysosome is a digestive organelle with a spherical shape and acidic environment in eukaryotic cells [95]. Lysosome participate in macromolecule digestion, energy balance, and angiogenesis [96, 97]. Lysosome defections are the cause of cardiovascular disease, neurodegenerative diseases, cancer, and Alzheimer's disease [29, 98, 99]. In recent years, researchers have been continuously designing lysosome-targeting CDs [100–105].

The CDs are a fast targeting agent for lysosome imaging through clathrin-mediated endocytosis. Detecting lysosomal

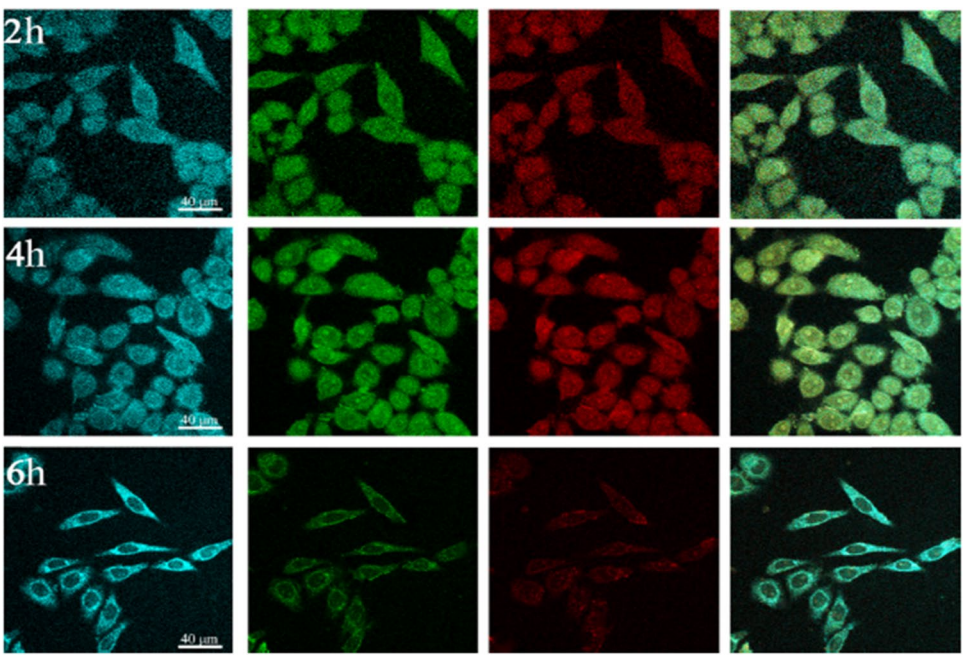

Fig. 2 Confocal fluorescence images of HeLa cells treated with prepared CDs for 2, 4, and 6 h. The 1–4 columns showed different excitation wavelengths at 405, 488, and 561 nm, Reproduced with permission from ref [87]. Copyright 2020 American Chemical Society

polarity can help to better understand the physiological and pathological processes of lysosomes. Moreover, the CDs show that an obvious fluorescence intensity decreases with the increase of polarity with the addition of dithiothreitol (DTT) that stimulates polarity changes in living cells (Fig. 3A). Therefore, the mentioned CDs were used successfully in monitoring the polarity of lysosomes [106]. New finding indicates that the morpholine group in the chemical structure of CDs serves as a targeting agent for lysosome imaging. These CDs particularly accumulate in the lysosome through the endocytic pathway and are able to long-time tracking of lysosomes in live cells. Figure 3B exposes bright orange fluorescence in the live cells when the green emission of the CDs was merged with the red emission of the LysoTracker Deep dye. In addition, the CDs show location conformity with the LysoTracker Deep Red during lysosome staining [45]. New CDs prepared from the rose bengal and polyethyleneimine via one-step hydrothermal procedure amazingly possess an intrinsic affinity to the lysosome. The image (Fig. 3C) shows the rapid entrance of prepared CDs into the cells within 10 min. Moreover, they accumulated in the lysosomes organelle and emitted strong localized fluorescence after the following 30 min. Long-term imaging, lack of leakage, ultrahigh photoluminescence efficiency, and low cytotoxicity are excellent properties of these CDs as a proven alternative for common commercial probes [107]. The CDs were prepared from selenocysteine as a precursor using the hydrothermal method and then modified with morpholine. Obtained CDs prevent lysosomes from the high amount of •OH and are introduced for treating •OH-related inflammation [108].

Briefly, CD modification with morpholine and amine groups is utilized for specific lysosome targeting. However, amino groups show affinity to the ER that faced its specificity to the lysosome with unresolved challenges. The cells uptake CDs through energy-dependent, micropinocytosis, caveolae-mediated, and clathrin-mediated pathways. CDs with various functional groups can be transiently localized in lysosomes.

Nucleus

The nucleus is the center of cellular metabolism, activity, and many disorders such as cancer. Detail imaging and staining of the nucleus are one of the most important biological and clinical issues because our knowledge about the nucleus is incomplete for its desired manipulation. Specific imaging of the nucleus is necessary for targeted gene therapy and drug delivery, especially cancer therapy. In addition to its potential for drug loading and drug delivery, the CDs have been found to be applicable in nucleus imaging as a specific and stable fluorescent probe [109–112].

The high water-soluble and nontoxic CDs are synthesized by a hydrothermal approach for bioimaging applications. The proposed mechanism for the nucleus targeting potential of reported CDs (Fig. 4A) is related to its positive surface charge, which creates electrostatic interactions with DNA macromolecules existing in the nucleus [109].

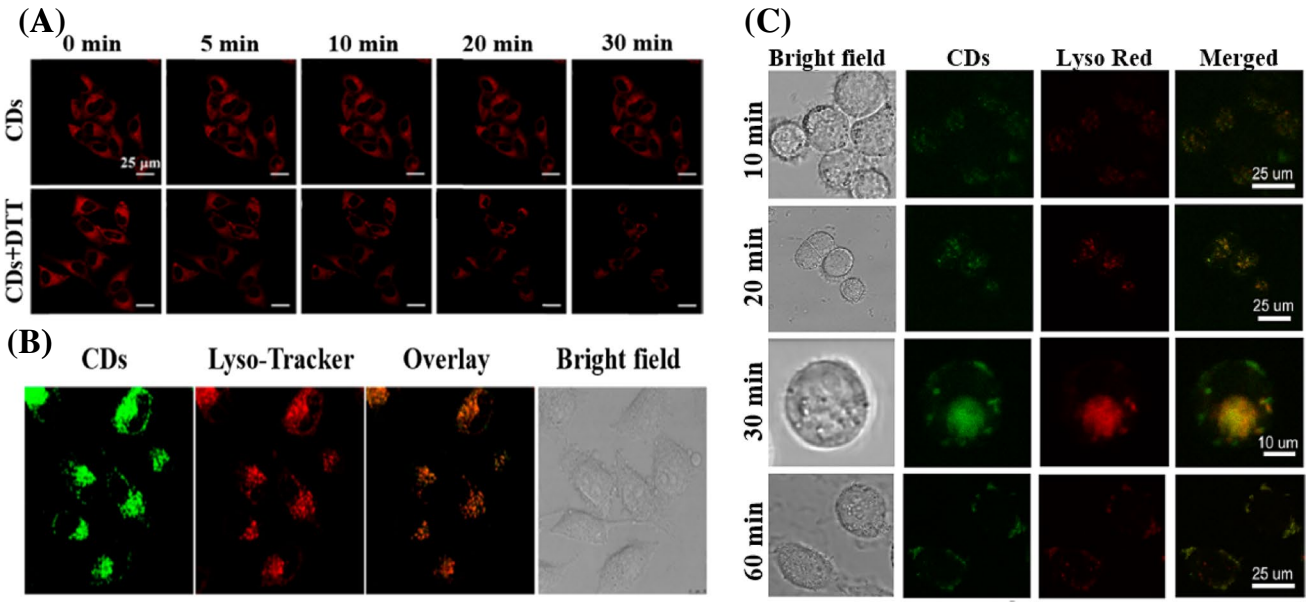

Fig. 3 **A** CLSM images of HeLa cells treated with CDs and CDs + DTT, Reproduced with permission from ref [106]. Copyright 2020 American Chemical Society. (**B**) The comparative images of CDs and Lyso-Tracker Red probe in live HeLa cells. Reproduced with permission from ref [45]. Copyright 2017 American Chemical Society. (**C**) Lysosomal imaging of the CDs in the HL-7702 cell line. Reproduced with permission from ref [107]. Copyright 2020 American Chemical Society

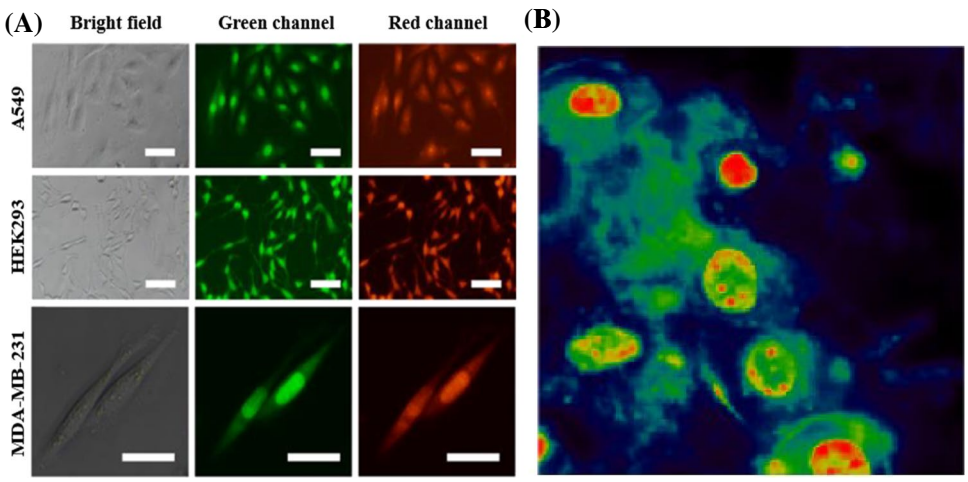

Fig. 4 **A** Fluorescence images of A549, HEK293, and MDA-MB-231 cells treated with CDs, fluorescence signal accumulated in nuclear substance, especially in A549 and MDA-MB-231 cells, Reproduced with permission from ref [109]. Copyright 2021 Elsevier. (**B**) The nuclei of NIH/3T3 cells filled with CDs (red color). False colored maps of intensity. Reproduced with permission from ref [110]. Published under a CC BY license

In some cases, the physicochemical environment of the cell (L929 cells) causes a blue shift in the fluorescent emission of CDs. The lowest and highest intensity of CDs was observed in cytosol and nucleus (green and red color), respectively (Fig. 4B) [110]. For the first time, an electrostatic assembly between positive CDs and negative graphene oxide (GO) provides a new biocompatible probe of the nucleus without significant affinity to the cytoplasm. GO nano-sheets do not quench CD fluorescent emission after assembly. These electrostatic interactions of CD and GO moderate the electrical charge of the final nano-structure, which results in selective cell nucleus labeling [111].

There are no particular and proven methods for selective labeling of the nucleus by using CDs. According to the previous report, the zwitterionic surfaces of CDs can specify their attachment to the nucleus. In a more complex way, surface functionalization of CDs is a certain approach of nucleus targeting, but this mechanism is also not precisely characterized and understood. It is obvious that the utility of CDs in nucleus imaging is in its beginning steps and is a very attractive field for interested researchers.

Nucleolus

Ribosomes synthesize all proteins needed by the cell that the nucleolus is responsible for the production of ribosomes [113]. Proteins are the functional form of cellular molecules. Therefore, the imaging of the nucleolus provides an overview of the cellular status and metabolism [114]. Immunohistochemistry (IHC) [115], fluorescence in situ hybridization (FISH) [116], and silver staining [117] are the most common methods for morphological evaluation of nucleolus that are served for fixed cell lines. Although organic fluorophores such as SYTO RNA [118] are utilized in both fixed and living cell imaging [119], they suffer from photobleaching during the nucleolus imaging process. Recent reports confirm the competence of CDs as wash-free, high-resolution, and high-quality nucleolar imaging probe with a high affinity to the nucleolus (Fig. 5A) [81]. Doping of fluorine element into the CD structure creates a new nucleolus and tunneling nano-tube (TNT) staining agent with the high photoluminescence quantum yield (56%), low toxicity, anti-photobleaching, and good water solubility (Fig. 5B) [120].

In summary, the affinity of CDs to interaction with nucleolus RNAs and ribosomes is the main reason for their application in nucleolus labeling [68, 120], which is related to noncovalent interactions. Although the subcellular labeling, the use of CDs in critical nucleolus diagnostic such as immune activation processes, transformation processes, and chemo-drug treatment are not reported, which are very attractive to examination.

Mitochondrion

The mitochondrion is the factory of energy production in mammalian cells by the creation of adenosine triphosphate (ATP) as a common form of energy in live cells [121]. Therefore any defect in mitochondrion causes significant disorders such as cardiac dysfunction, Alzheimer's, and Parkinson's diseases [122]. The mitochondrion has an internal negative charge, positive surface charge, and an internal alkaline environment (pH = 8) [123, 124]. Hence, two strategies are possible for specific imaging of mitochondrion: one is a modification with triphenylphosphonium (TPP) or targeting peptides, and the other way is to synthesize lipophilic labels containing positive surface groups such as ammonium, pyridine, and rhodamine [51].

The TPP ligands are practically utilized for the improvement of CD affinity to the mitochondria [125]. In spite of appropriate targeted imaging of mitochondria using these CDs, TPP shows high toxicity against various cell lines. On the other side, some works are in progress to obtain CDs with intrinsic mitochondrial targeting property [42, 123,

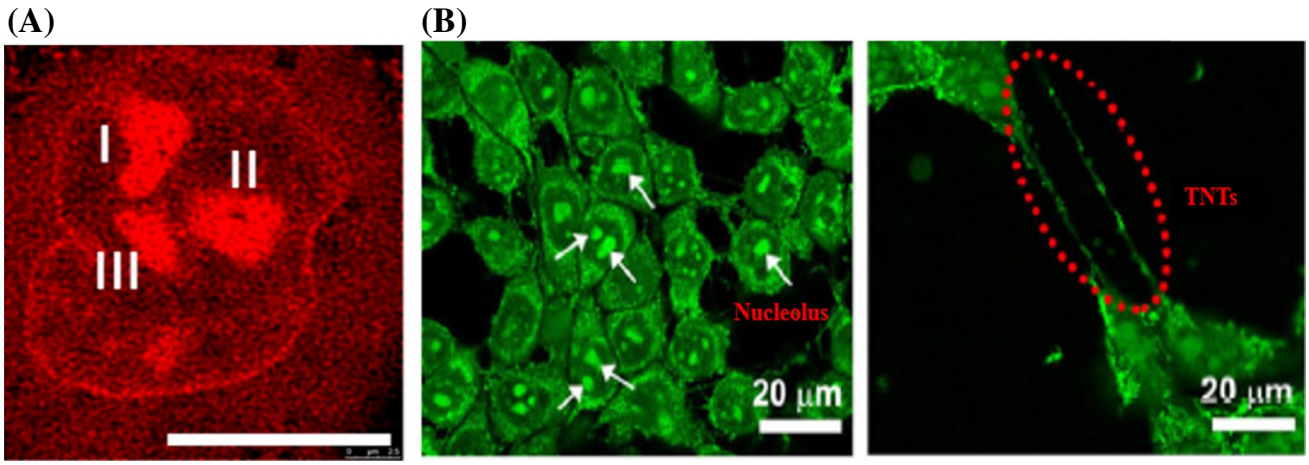

Fig. 5 **A** The confocal image of the nucleolus of A549 (I, II, and III) cells targeted by CDs, Reproduced with permission from ref [81]. Copyright 2019 American Chemical Society. (**B**) CLSM images of living 4T1 cells treated with CDs, the nucleolus (left), and tunneling nano-tubes (right) were visualized with sharp fluorescent signals. Reproduced with permission from ref [120]. Copyright 2019 Springer

126]. Long-term photostable, water-soluble, mono-sized, and biocompatible CDs were synthesized with intrinsic mitochondrial affinity and tunable long-wavelength fluorescence emission from green to red colors. A high-resolution mitochondrial image of HeLa cells was obtained using as-synthesized CDs (Fig. 6A) [127]. The fast and simple microwave-assisted method was applied as a synthesis method of new excellent CDs with shuttling label features between the mitochondria and the nucleolus. These positive CDs prefer to accumulate in mitochondria with negative membrane within the healthy cells. However, in the case of damaged cells, such as inhibition of the cell metabolism by reactive oxygen species (ROS) agents such as H_2O_2, the negative charge of mitochondria decreases, and CDs move out from mitochondria and localize into the nucleolus. Amazingly, if the damaged cell succeeds in recovering itself in the presence of powerful antioxidants such as ascorbic acid (AA), the negative charge of mitochondria will recover too, which triggers the return of CDs to the mitochondria (Fig. 6B). In this way, the viability of a particular cell can be easily visualized [128].

Endoplasmic reticulum

The main functionality of ER in the cell is the formation of proteins, transporting of protein, synthesis and storage of lipids, storage and regulation of calcium, and glucose metabolism. Therefore, ER plays a vital role in cell metabolism and regulation [129]. Polarity is one of the most important properties of healthy cells, and it is responsible for lots of cellular functions and metabolism. ER can affect cell polarity and consequently cell functionality via protein post

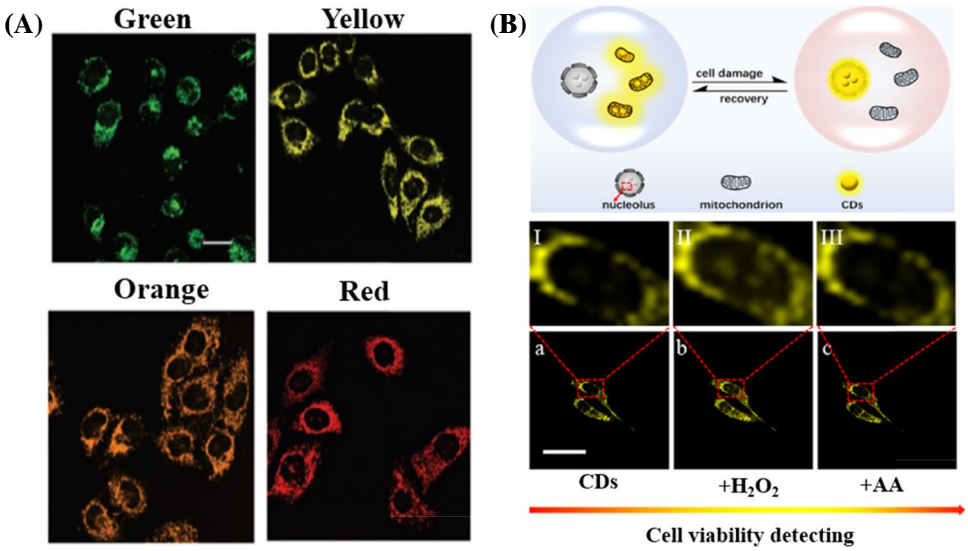

Fig. 6 **A** Confocal images of HeLa cells incubated with green, yellow, orange, and red CDs, Reproduced with permission from ref [127]. Copyright 20,193 Wiley–VCH. (**B**) Shuttling of CDs between mitochondria and the nucleolus, (top) schematic and (bottom) fluorescent images of HeLa cells. Reproduced with permission from ref [128]. Copyright 2020 American Chemical Society

translational modification, the transformation of particular proteins, and the synthesis of secretory proteins. As a result, any disorder in ER polarity can be a significant symptom of human diseases such as diabetes and Alzheimer's [130]. Accordingly, clear imaging of ER provides proven information about cell functionality and human diseases.

Dual emissive CDs for ER labeling are obtained from o-phenylenediamine (OPD) and lysine. Adding lysine into the flask of OPD carbonization reaction strongly suppressed the reaction and caused emission shifting from green to blue. The synthesized CDs have entered the ER lumen via lipid raft-mediated endocytosis pathway because of their lipophilicity and electrophilicity. Introduced CDs are responsive to the changes of ER polarity in living cells that indicate their potential to the imaging of the ER stresses [131].

Briefly, CDs can electively visualize ER and provide sufficient morphological information. More information about the activity of ER and other organelles can be obtained via the aggregation and fluorescence responses of the CDs inside ER to environmental differences, including pH values within these organelles.

Lipid droplet

Lipid droplets (LDs) are a hydrophobic core made from lipid covered by a monolayer of phospholipid membrane [132]. LDs roles in the cell are lipid storage, membrane synthesis, and transportation, so it is supposed to be related to lipid metabolic diseases such as obesity, atherosclerosis, and cancer [133]. Consequently, imaging lipid droplets with CDs is an advantageous method of tracking cellular lipid metabolism and related diseases.

The biocompatible and amphiphilic CDs were synthesized via the hydrothermal method for LD imaging. The high cell viability, photostability, intracellular retention ability, and long-term ability to LD tracking are the highlight properties of prepared CDs. After six passages, selective fluorescence CDs can still be observed in LDs in the cytoplasm of the cells (Fig. 7A). The imaging of autophagy in the catabolic process and the effect of atorvastatin (a typical drug for lowering lipid levels) on hepatocyte cells are accomplished by reported CD [134]. The CDs with the ability of intrinsic LD targeting are obtained from 4-piperidinoaniline (PA) as a lipophilic reactant. By using these CDs, the dynamic behavior of LDs and also fatty liver disease-like changes in LD are visualized (Fig. 7B) [135].

Detecting and imaging of intracellular pH

Similar to all chemical reactions, intracellular pH values play a central role in cellular functions, including metabolism pathways, growth, proliferation, apoptosis, and disease. A little variation in the cellular pH can be a signal of particular metabolic reactions, disorders, and diseases such as Alzheimer's, cancer, and stroke [136, 137].

Application of common nano-size pH probes such as organic dyes and QDs [138–140] are restricted by their disability to cell entrance and high toxicity. The CDs are new alternatives for overcoming all previous obstacles [141, 142]. A biocompatible, tunable, and multicolor CD was prepared from ammonium persulfate, glucose, and ethylenediamine via the hydrothermal method. Recently, designed CDs could be used as a fluorescence platform to monitor pH fluctuations in living cells. The HepG2 cells labeled with these CDs emitted multi-color fluorescence at pH 5.0. As the pH increases from 5 to 9, the fluorescent brightness labeled cells decreases. Therefore, the changes in the brightness of CDs in the living cells can be translated to the intracellular pH variation. The prepared CDs are able to easily penetrate into the living cells and simultaneously visualize the pH statements of the cells (Fig. 8A) [136]. Also, the pH-responsive nitrogen- and chloride-doped CDs were synthesized by choline chloride and glycerin as an intracellular pH sensing probe (Fig. 8B) [143]. Another hydrothermal synthesis of nitrogen-rich CDs as pH sensor from melamine and triethanolamine was recently reported. A wide range of sensing, low cell cytotoxicity, and excellent biocompatibility were

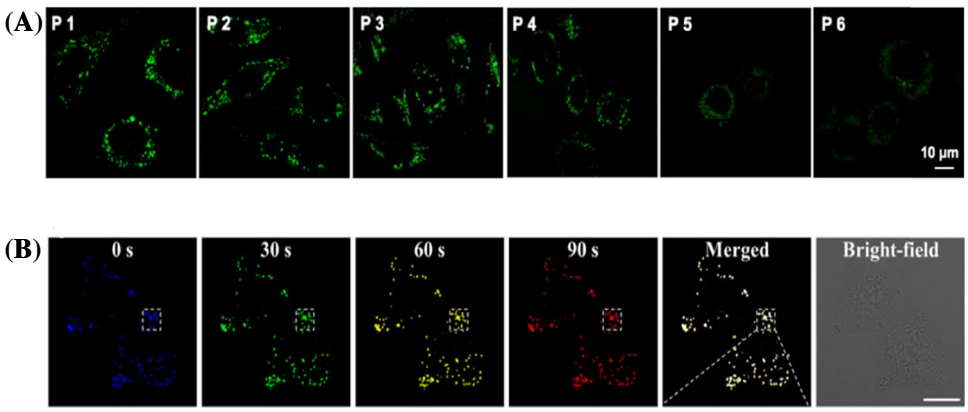

Fig. 7 **A** Confocal images of LoVo cells treated with CDs at different passages. CDs: excitation at 405 nm, Reproduced with permission from ref [134]. Copyright 2021 American Chemical Society. (**B**) Monitoring of the LD movement by PA CDs: the movement of LDs at 0, 30, 60, and 90 s is illustrated by four different colors, and the merged of all images. Reproduced with permission from ref [135]. Copyright 2021 American Chemical Society

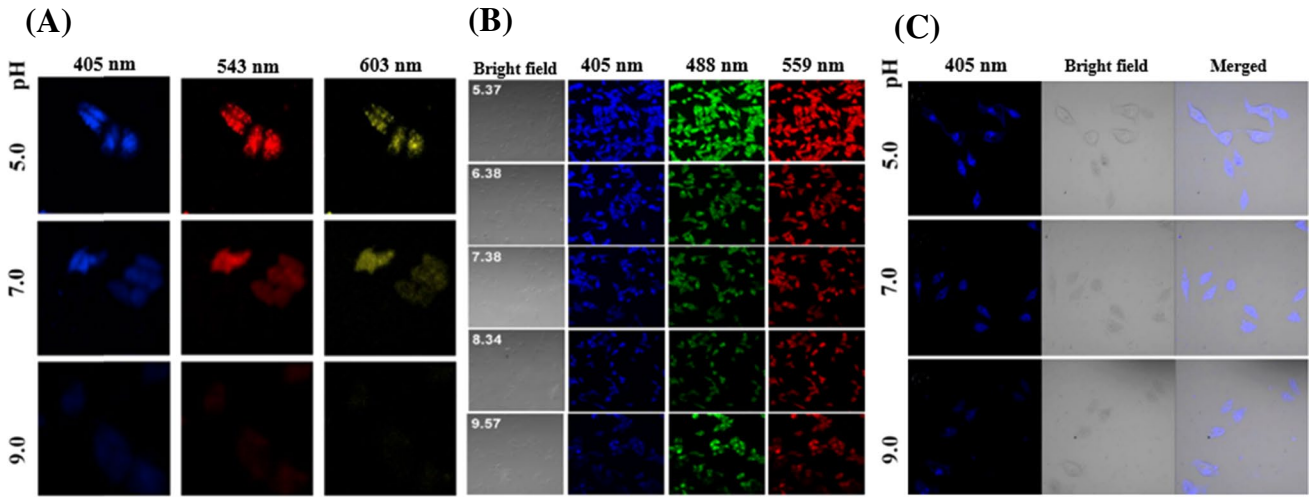

Fig. 8 **A** Confocal images of HePG2 cells treated with CDs at pH (5.0, 7.0, 9.0), Reproduced with permission from ref [136]. Copyright 2020 Elsevier. (**B**) Confocal images of HeLa cell incubation with CDs at pH (5.37, 6.38, 7.38, 8.34, and 9.57). Reproduced with permission from ref [143]. Copyright 2018 American Chemical Society. (**C**) Confocal images of T24 cells treated with CDs at pH (5.0, 7.0, 9.0). Reproduced with permission from ref [144]. Copyright 2016 Elsevier

the remarkable properties of prepared CDs that confirm via imaging of pH sensing in live T24 cells (Fig. 8C) [144].

In spite of the proposed mechanism of pH imaging by CDs, including protonation or deprotonation, energy level variation, particle aggregation, protective shell, and proton transfer, there is a priority to exact explanation about this phenomenon [145].

Detecting and imaging of intracellular ion

Heavy metal ions are toxic to life in nature, but the main concern about heavy metals relates to their unknown and intricate effects on living organisms. So, any method of detecting this heavy metal ion has its own priority for researchers [146, 147]. Functionalized CDs are one of the recent tendencies to metal ion detection [49, 148]. The attractive CDs with high sensitivity to Fe^{3+} were obtained via microwave pyrolysis within just 4 min. As an intrinsic fluorescence probe, CDs practically visualize intracellular Fe^{3+} in live HeLa cells (Fig. 9A) [149]. Also, the CDs prepared from microalgal biomass are a candidate as potent endogenous imaging labels of Hg (II)- and Cr (VI)-contaminated live cells (Fig. 9B) [150].

The reported mechanisms of heavy metal detection by CDs are coordination/complexation, inner filter effect (IFE), light-induced electron transfer (LET), and ion aggregation [151]. CDs have a great potential for visualization of other heavy metal ions such as Cr and As.

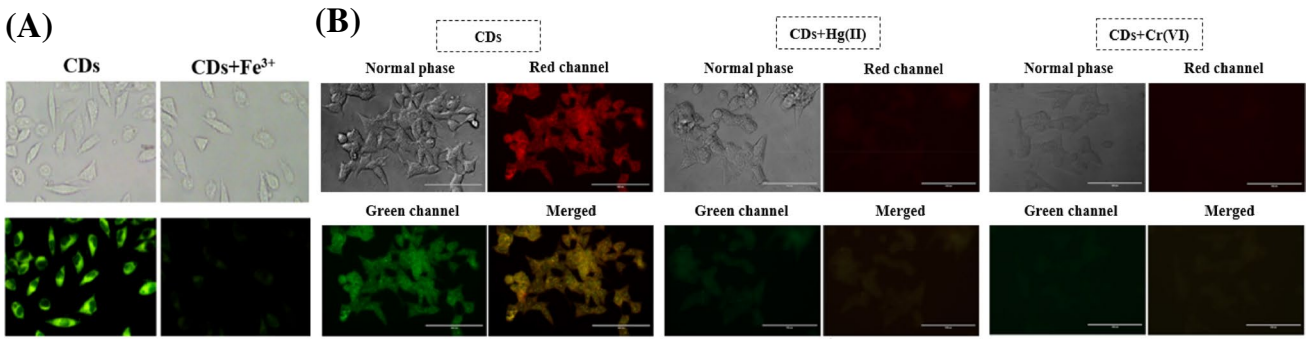

Fig. 9 **A** Bright-field transmission images and their corresponding fluorescent microscopy images of HeLa cells that were incubated with CDs and then Fe3+, Reproduced with permission from ref [149]. Copyright 2018 Springer. (**B**) Cell imaging of HEK-293 cell line after treatment of 50 μg/mL of CDs, 100 μM Hg (II), and 100 μM Cr (VI). Reproduced with permission from ref [150]. Copyright 2018 Elsevier

Detecting and imaging of intracellular small molecule

High-resolution imaging of small cellular molecules such as glutathione and dopamine always provides more details about biochemical pathways, the mechanism of cellular activity, and the pathophysiology of disease progression [152, 153]. The new NIR fluorescence CDs can be directly used for the quantitative evaluation of H_2S. More surprising, this kind of CD could specifically be used for imaging of the cell membrane H_2S transporting. As shown in Fig. 10A, the MCF-7 cells incubated only with CDs emit a bright red fluorescence from the cell membrane, while the fluorescence intensity of the NIR channel decreases obviously in the presence of the H_2S. In addition to the labeling of the cell membrane by CDs, more detail about the signal pathways and cell–cell communications are accessible by visualization of gaseous signal molecule transportation across the cell membrane. The mechanism of fluorescent quenching and affinity to the H_2S by CDs are not illustrated yet [154]. Simple and fast preparation of CDs from L-tartaric acid and triethylenetetramine was examined via the microwave-assisted method. Fluorescent quenching is the mechanism of metronidazole (MNZ) detection by these biocompatible CDs. Accordingly, CDs are a potent tool for cell imaging and MNZ detection (Fig. 10B) [155]. Also, CD-based fluorescent nano-probes for intracellular biothiols (cysteine, homocysteine, and glutathione) imaging in living cells were introduced due to their appropriate biocompatibility [156, 157].

Detecting and imaging of intracellular protein

The imaging of protein distribution and tracking of their cellular movement is necessary for a complete understanding of biological pathways and disorders [158]. Conjugation of Au nano-rods (AuNR) and red-emissive CDs (RCDs) provides a specific fluorescent label for caspase-1 activity assay (Fig. 11A). The emission of fluorescent energy occurs by CD and adsorbs by the Au nano-rods via surface energy transfer (SET) phenomena. The obtained fluorescent probe shows high sensitivity, specificity, and stability for in situ monitoring and imaging of the caspase-1 activity level in the living cells (Fig. 11B) [159]. As an imaging agent, CDs show selective emission response to cytochrome C (cyt-c) via an unclear mechanism. The HeLa cells were incubated with synthesized CDs and dexamethasone for various times. The dexamethasone triggers cyt-c releasing from the mitochondria and simultaneously the beginning of the apoptosis process, which could be monitored by confocal fluorescence imaging (Fig. 11C) [143].

Table 1 shows precursors, emission color, size, biocompatibility, and important features and targets of CDs for live-cell imaging reported in the literature. In this table, we have tried to summarize the latest published articles in this field during the last few years.

Conclusion and future perspective

Cellular imaging is intricate and expensive, but it is one of the most valid techniques for understanding metabolic pathways and the mechanism of disease. The unlimited amounts

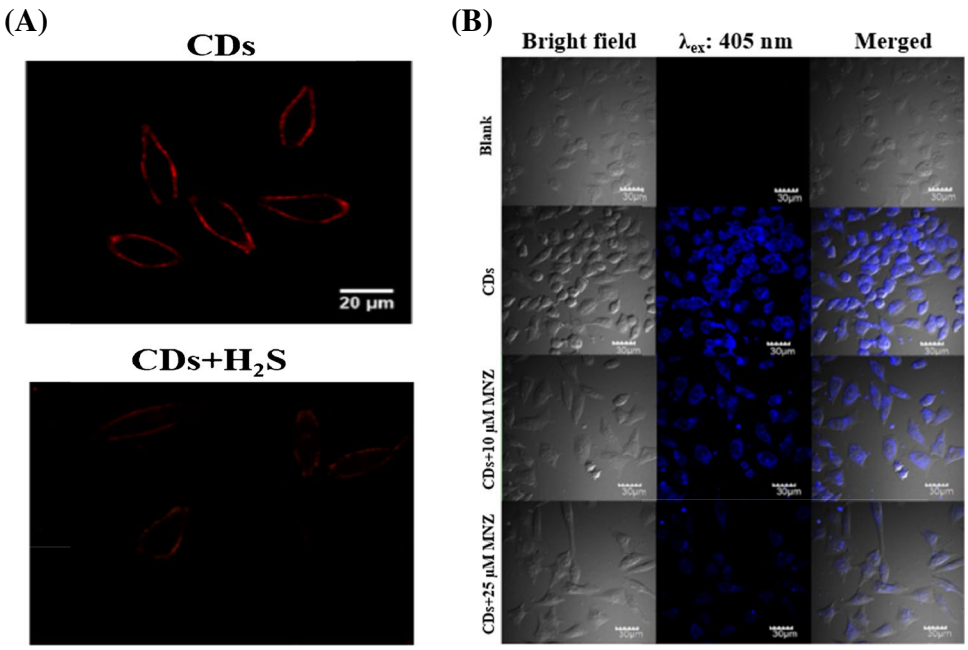

Fig. 10 **A** Red channel images (λex = 640 nm) of MCF-7 cells incubated with CDs (top) and CDs + NaHS (sodium hydrosulfide) (bottom), Reproduced with permission from ref [154]. Copyright 2021 Elsevier. (**B**) CLSM images of MCF-7 cells treated with CDs in with or no MNZ. Reproduced with permission from ref [155]. Copyright 2020 Elsevier

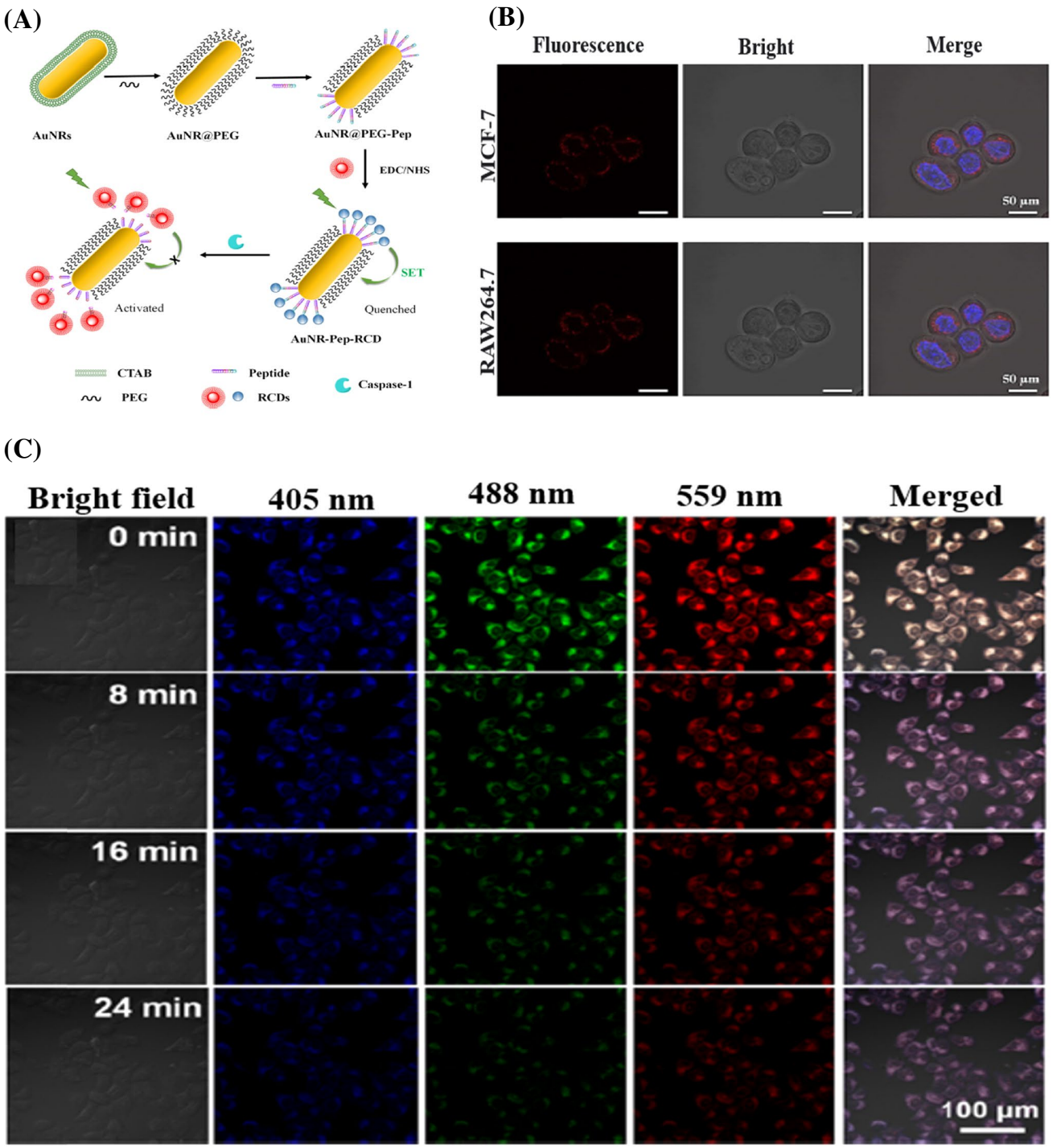

Fig. 11 **A** Schematic synthesis procedure of the caspase-1 and its response mechanism of the AuNR-Pep-RCD nano-probe. (**B**) Confocal images of MCF-7 and RAW264.7 cells treated with AuNR-Pep-RCD. The red color is related to the nano-probe response to active caspase-1, and the blue color comes from Hoechst 33,342 for cellular nucleus staining, Reproduced with permission from ref [159]. Copyright 2021 Elsevier. (**C**) Confocal fluorescence images of HeLa cells incubated with CDs for 5 h followed by further incubation for 0, 8, 16, and 24 min in the presence of dexamethasone. Reproduced with permission from ref [143]. Copyright 2018 American Chemical Society

Table 1 An overview of the use of different CDs for in vitro live-cell imaging

Precursors	Emission				Size (nm)	Biocompatibility Viability > 80% (Mostly by MTT assay)	Features								Imaging target	Ref.
	Blue	Green	Yellow	Red			Brightness	Fluorogenicity	Multicolor	Photoblinking	Photostability	Red & NIR	Stimuli-responsive	Up-conversion		
Sugarcane Ethylenediamine	■	■	■	■	10.7	---			●		●	●			Cytoplasm	[75]
Lemon juice Ethylenediamine	■	■		■	3	0-2 mg/mL	●				●				Cytoplasm	[89]
Urea Sodium alginate	■	■		■	3.4	0-900 μg/mL CCK-8			●						Cytoplasm	[87]
H_2O_2 NH_3 H_2O Ammonium citrate		■			3.5	CCK-8 assay 0-100 μg/mL	●							●	Cytoplasm	[88]
Citric acid 2,6-Diaminopyridine	■	■			2.1	0-5 mg/mL			●		●				Cytoplasm	[90]
Scallion	■				3.2	0–10 μg/mL	●				●		●		Cytoplasm	[91]
Waste polyolefin		■		■	2.5	0–200 μg/mL					●	●	●		Cytoplasm	[92]
Cysteine Dopamine	■				2–3	0–50 μg/mL		●	●	●					Cytoplasm	[93]
Arginine Citric acid Ethylenediamine	■	■		■	1-4.5	AlmarBlue assay 0.25 mg/mL	●		●				●		Cytoplasm	[94]
Citric acid Ethylenediamine Diethylenetriamine Tetraethylenepentamine		■		■	3-5	0-800 μg/mL	●				●	●			Cytoplasm, Nucleus	[160]
Graphite rods		■			6	0-1 mg/mL					●		●	●	Cytoplasm	[161]
p-Phenylenediamine Thiourea				■	3-5	1-160 μg/mL					●	●			Cytoplasm	[162]
Citric acid Polyethylenimine 4-(2-aminoethyl) morpholine		■		■	4	CCK-8 assay 0-900 μg/mL		●	●		●	●			Lysosome	[45]
*PEG_{2000} ([AMIm][PF6])		■			10	0–100 μg/mL					●		●		Lysosome	[100]
Styrylcyanine dye o-Phenylenediamine			■		3	0-1 mg/mL					●		●		Lysosome	[101]
Spermine Rose bengal		■			2.2	0-800 μg/mL	●				●				Lysosome	[102]
Benzendiamine dihydrochloride			■		1.8	0-50 μg/mL	●				●				Lysosome	[103]
Shiitake mushroom	■	■			4.2	0.5- 4 mg/mL	●		●						Lysosome	[104]
Chloranil Triethylenetetramine		■			3.3- 7.8	CCK-8 assay 0.1–50 μg/mL	●				●				Lysosome	[105]
N-Phenyl-o- phenylenediamine				■	2.2	0–80 μg/mL					●	●	●		Lysosome	[106]
Rose Bengal Polyethylenimine		■			30–50	0-1 mg/mL	●		●		●				Lysosome	[107]
Selenocystine	■			■	2.7	0–100 μg/mL		●	●		●	●			Lysosome	[108]

Table 1 (continued)

N-phenyl-p-phenylenediamine	■			■	3.2	CCK-8 assay 0-100 μg/mL						●	●		Lysosome	[163]
Citric acid Polyethyleneimine		■		■	6.21	0-500 μg/mL	●				●	●			Nucleus	[109]
Tris Betaine hydrochloride				■	7	---					●	●			Nucleus	[110]
Tris Betaine hydrochloride		■		■	4–9	0-100 μg/mL			●			●			Nucleus	[111]
Citric acid Polyethylenimine	■				2.6	0-5 mg/mL	●				●				Nucleus	[112]
Urea Citric acid Ammonium fluoride				■	2.6	0–200 μg/mL						●		●	Nucleolus	[66]
p-Aminoazobenzene				■	4	0-100 μg/mL	●	●				●		●	Nucleolus	[68]
Nickel chloride p-Phenylenediamine				■	2.9	0–50 μg/mL		●			●	●			Nucleolus	[81]
Glycine 2,4-Difluorobenzoic acid		■			5	---	●	●			●				Nucleolus	[120]
Beer residue	■				4	---						●		●	Nucleolus	[164]
Malic acid Ethylenediamine	■	■	■		6-15	---	●		●	●	●				Mitochondrion	[42]
Citric acid m-Aminophenol		■	■	■	1.9-3.3	0–200 μg/mL	●		●		●	●			Mitochondrion	[127]
Citric acid N, N-Dimethylaniline			■	■	3.7	0–60 μg/mL		●	●		●	●	●		Mitochondrion	[128]
Lysine o-phenylenediamine		■			2.9	40 - 500 μg/mL			●		●				Endoplasmic reticulum	[131]
o-Phenylenediamine		■		■	<10	0-2 mg/mL		●			●	●			Lipid droplet	[134]
4-piperidinoaniline				■	2.1	0-30 μg/mL					●	●			Lipid droplet	[135]
Glucose Ethylenediamine Ammonium persulfate	■	■	■	■	4–10	0-0.8 mg/mL			●		●		●	●	pH	[136]
L-arginin Ascorbic acid Fluoresceinamine		■			5–10	MTS assay 100–800 μg/mL					●		●	●	pH	[137]
m-Phenylenediamine H_2SO_4 C_2H_5OH		■			1.8-3	0-60 μg/mL	●				●		●		pH	[142]
Melamine Triethanolamine	■				5	0-5 mg/mL							●		pH	[144]
Urea Glycerine Choline chloride	■	■		■	3.8	0- 5 mg/mL	●		●						pH & Protein	[143]
Plant *Tulsi-Ocimum sanctum*	■	■		■	3	0–200 μg/mL			●		●		●		Ion	[148]
Citric acid Lanthanum chloride Methylamine hydrochloride		■			2–6	---		●			●		●		Ion	[149]

Table 1 (continued)

Micro-algae *Dunaliella salina*					2-8	0-5 mg/mL					●	●			Ion	[150]
Trisodium citrate Sodiumthiosulfate					5	0-15 mg/mL	●	●	●			●	●		Small molecule	[77]
Porcine pancreatic lipase					1-5	0–100 μg/mL	●						●		Small molecule	[79]
Methyl blue					2.3	0-2 mg/mL	●			●	●	●			Small molecule	[152]
Plant *Wedelia Trilobata*					2.8	CCK-8 assay 50-400 μg/mL					●	●	●		Small molecule	[153]
Azure A chloride Copper gluconate					4.5	0-5 mg/mL						●	●		Small molecule	[154]
L-tartaric acid Triethyleneteramine					2.5	0-5 mg/mL	●		●		●				Small molecule	[155]
3-diethylaminophenol					2.94	0-40 μg/mL							●		Small molecule	[156]
Calcon-carboxylic acid					5.1	CCK-8 assay 0-80 μg/mL							●		Small molecule	[157]
Glycerol Ethylenediamine					5	---					●		●		Small molecule	[165]
*DBP Citric acid					21	0-200 μg/mL			●			●			Protein	[158]
Urea Citric acid					2.5	0-5 nM			●		●	●	●		Protein	[159]

CCK-8 Cell Counting Kit-8, *DBP* 20-diamino-1,10-binaphthalene, *([AMIm][PF6])* 1-allyl-3-methylimidazolium hexafluorophosphate, PEG_{2000} polyethylene glycol-2000

*Brightness: QY > 15%

of biological molecules are synthesized, modified, and transformed per second in the cells, interfering in targeted chemical labels. CDs can answer the highly variable and streaming nature of cells by the possibility of preparation by unlimited and cheap precursors from pure citric acid to contaminant waste water. Therefore, a wide variety of surface chemical groups and surface modifications are available in the designation of CDs as a selective probe for cellular organelles and bioactive molecules. High-resolution imaging, stable fluorescent emitting, ability to cell penetration, surface multifunctional capabilities, biocompatibility, low-cost synthetic, and low toxicity are the additional advantages of CDs against the common dyes and nano-probes. The newest progress in in vitro live-cell imaging based on CDs, including the whole cells, cell organelles, pH, ions, molecules, and proteins imaging, are elaborately presented in this review. However, the fundamental mechanism of selective behavior of CDs against a particular organelle or biomolecule is not clearly reported. Undoubtedly, the future progress in cell imaging depends on the illustration of the mechanism of cellular and subcellular specific imaging by various chemically CDs. In spite of attempts to improve the targeting ability of CDs via post surface modification such as chemical conjugation with Au nano-rods, researchers are tending to achieve this goal by altering simple and low-cost reactions to synthesize CDs with intrinsic affinity to a particular target.

Declarations

Ethics approval Not applicable.

Conflict of interest The authors declare no competing interests.

References

1. Arandian A et al (2019) Optical imaging approaches to monitor static and dynamic cell-on-chip platforms: a tutorial review. Small 15(28):1900737
2. Nowzari, F., et al 2021 *Three-dimensional imaging in stem cell-based researches.* Frontiers in Veterinary Science, **8**
3. Ali H, Ghosh S, Jana NR (2020) Fluorescent carbon dots as intracellular imaging probes. Wiley Interdisciplinary Reviews: Nanomedicine and Nanobiotechnology 12(4):e1617
4. Kiepas A et al (2020) Optimizing live-cell fluorescence imaging conditions to minimize phototoxicity. Journal of cell science 133(4):242834

5. Jin D et al (2018) Nanoparticles for super-resolution microscopy and single-molecule tracking. Nat Methods 15(6):415–423
6. Xu, Q., et al 2021 *Quantum dots on cell imaging and safety issues.* Journal of Materials Chemistry B
7. Wu, F.-G 2020 *Fluorescent materials for cell imaging*. Springer
8. Hakiminia F et al (2016) Adjustment of local conformational flexibility and accessible surface area alterations of Serine128 and Valine183 in mnemiopsin. J Mol Struct 1117:287–292
9. Hakiminia F et al (2016) Determination of structural elements on the folding reaction of mnemiopsin by spectroscopic techniques. Spectrochim Acta Part A Mol Biomol Spectrosc 158:49–55
10. Hakiminia F, Ranjbar B, Khalifeh K (2013) Kinetic and thermodynamic properties of Pseudomonas fluorescence lipase upon addition of proline. Int J Biol Macromol 55:123–126
11. Ganjalikhany MR et al (2010) Roles of trehalose and magnesium sulfate on structural and functional stability of firefly luciferase. J Mol Catal B Enzym 62(2):127–132
12. Yousefi-Nejad M et al (2007) Expression, purification and immobilization of firefly luciferase on alkyl-substituted Sepharose 4B. Enzyme Microb Technol 40(4):740–746
13. Maghami P et al (2010) Relationship between stability and bioluminescence color of firefly luciferase. Photochem Photobiol Sci 9(3):376–383
14. Badoei-Dalfard A et al (2010) Enhanced activity and stability in the presence of organic solvents by increased active site polarity and stabilization of a surface loop in a metalloprotease. J Biochem 148(2):231–238
15. Traenkle B, Rothbauer U (2017) Under the microscope: single-domain antibodies for live-cell imaging and super-resolution microscopy. Front Immunol 8:1030
16. Klein T et al (2011) Live-cell dSTORM with SNAP-tag fusion proteins. Nat Methods 8(1):7–9
17. Behroodi E et al (2020) A combined 3D printing/CNC micromilling method to fabricate a large-scale microfluidic device with the small size 3D architectures: an application for tumor spheroid production. Sci Rep 10(1):1–14
18. Azizi A et al (2014) Surface plasmon resonance coupled circular dichroism of DNA–gold nanorods assembly. J Phys D: App Phys 47(31):315401
19. Rahimifard, M., et al 2021 *Assessment of cytotoxic effects of new derivatives of pyrazino [1, 2-a] benzimidazole on isolated human glioblastoma cells and mitochondria.* Life Sciences 120022
20. Azizi A et al (2014) Plasmonic circular dichroism study of DNA–gold nanoparticles bioconjugates. Plasmonics 9(2):273–281
21. Bonnet G et al (1999) Thermodynamic basis of the enhanced specificity of structured DNA probes. Proc Natl Acad Sci 96(11):6171–6176
22. Rahimi B et al (2021) The secretome of mesenchymal stem cells and oxidative stress: challenges and opportunities in cell-free regenerative medicine. Mol Biol Rep 48(7):5607–5619
23. Panahi M et al (2020) Cytoprotective effects of antioxidant supplementation on mesenchymal stem cell therapy. J Cell Physiol 235(10):6462–6495
24. Wang Y et al (2013) 3D super-resolution imaging with blinking quantum dots. Nano Lett 13(11):5233–5241
25. Xu J, Tehrani KF, Kner P (2015) Multicolor 3D super-resolution imaging by quantum dot stochastic optical reconstruction microscopy. ACS Nano 9(3):2917–2925
26. Dertinger T et al (2009) Fast, background-free, 3D super-resolution optical fluctuation imaging (SOFI). Proc Natl Acad Sci 106(52):22287–22292
27. Jaiswal JK et al (2004) Use of quantum dots for live cell imaging. Nat Methods 1(1):73–78
28. Rezaei Z, Ranjbar B (2017) Ultra-sensitive, rapid gold nanoparticle-quantum dot plexcitonic self-assembled aptamer-based nanobiosensor for the detection of human cardiac troponin I. Eng Life Sci 17(2):165–174
29. Ardekani LS et al (2019) Design and fabrication of a silver nanocluster-based aptasensor for lysozyme detection. Plasmonics 14(6):1765–1774
30. Verma NC et al (2021) Emergence of carbon nanodots as a probe for super-resolution microscopy. J Phys Chem C 125(3):1637–1653
31. Hou J et al (2016) Synthesis and formation mechanistic investigation of nitrogen-doped carbon dots with high quantum yields and yellowish-green fluorescence. Nanoscale 8(21):11185–11193
32. Xu Q et al (2015) Preparation of highly photoluminescent sulfur-doped carbon dots for Fe (III) detection. J Mater Chem A 3(2):542–546
33. Zhu S et al (2015) The photoluminescence mechanism in carbon dots (graphene quantum dots, carbon nanodots, and polymer dots): current state and future perspective. Nano Res 8(2):355–381
34. Zhao P, Zhu L (2018) Dispersibility of carbon dots in aqueous and/or organic solvents. Chem Commun 54(43):5401–5406
35. Liu D et al (2015) Generalized one-pot strategy enabling different surface functionalizations of carbon nanodots to produce dual emissions in alcohol–water binary systems. J Phys Chem C 119(31):17979–17987
36. Hallaji, Z., et al 2021 *Recent advances in the rational synthesis of red-emissive carbon dots for nanomedicine applications: a review.* FlatChem 100271
37. Bagheri Z et al (2018) Investigation the cytotoxicity and photo-induced toxicity of carbon dot on yeast cell. Ecotoxicol Environ Saf 161:245–250
38. Bagheri Z et al (2018) On-chip analysis of carbon dots effect on yeast replicative lifespan. Anal Chim Acta 1033:119–127
39. Jiang K et al (2015) Red, green, and blue luminescence by carbon dots: full-color emission tuning and multicolor cellular imaging. Angew Chem 127(18):5450–5453
40. Yao Z et al (2019) Full-color emissive carbon-dots targeting cell walls of onion for in situ imaging of heavy metal pollution. Analyst 144(11):3685–3690
41. Singh V et al (2018) Biocompatible fluorescent carbon quantum dots prepared from beetroot extract for in vivo live imaging in C elegans and BALB/c mice. J Mater Chem B 6(20):3366–3371
42. Zhi B et al (2018) Malic acid carbon dots: from super-resolution live-cell imaging to highly efficient separation. ACS Nano 12(6):5741–5752
43. Nandi, S., et al., *Lipid-bilayer dynamics probed by a carbon dot-phospholipid conjugate.* Biophysical journal, 2016. **110**(9).
44. Du F et al (2015) Multicolor nitrogen-doped carbon dots for live cell imaging. J Biomed Nanotechnol 11(5):780–788
45. Wu L et al (2017) Morpholine derivative-functionalized carbon dots-based fluorescent probe for highly selective lysosomal imaging in living cells. ACS Appl Mater Interfaces 9(34):28222–28232
46. Zhang QQ et al (2018) A functional preservation strategy for the production of highly photoluminescent emerald carbon dots for lysosome targeting and lysosomal pH imaging. Nanoscale 10(30):14705–14711
47. Kang Y-F et al (2015) Nucleus-staining with biomolecule-mimicking nitrogen-doped carbon dots prepared by a fast neutralization heat strategy. Chem Commun 51(95):16956–16959
48. Jung YK, Shin E, Kim B-S (2015) Cell nucleus-targeting zwitterionic carbon dots. Sci Rep 5(1):1–9
49. Bagheri Z et al (2017) New insight into the concept of carbonization degree in synthesis of carbon dots to achieve facile smartphone based sensing platform. Sci Rep 7(1):1–11

50. Li H et al (2020) Recent advances in carbon dots for bioimaging applications. Nanoscale Horizons 5(2):218–234
51. Zhang X et al (2021) Advances in organelle-targeting carbon dots. Fullerenes, Nanotubes, Carbon Nanostruct 29(5):394–406
52. Unnikrishnan B et al (2020) Fluorescent carbon dots for selective labeling of subcellular organelles. ACS Omega 5(20):11248–11261
53. Guo H, Wang L (2021) Recent progress in the development of carbon quantum dots for cell imaging. Oxford Open Materials Science 1(1):itab001
54. Du J et al (2019) Carbon dots for in vivo bioimaging and theranostics. Small 15(32):1805087
55. Dalal C et al (2021) Fluorescent carbon nano-onion as bioimaging probe. ACS Appl Bio Mater 4(1):252–266
56. Wu H et al (2021) Recent advance in carbon dots: from properties to applications. Chin J Chem 39(5):1364–1388
57. Ray, P., P. Moitra, and D. Pan 2021 *Emerging theranostic applications of carbon dots and its variants.* View, 20200089
58. Zhang, M., et al 2020 *When rare earth meets carbon nanodots: mechanisms, applications and outlook.* Chemical Society Reviews
59. Kurian, M. and A. Paul 2021 *Recent trends in the use of green sources for carbon dot synthesis—a short review.* Carbon Trends 100032
60. Huo F et al (2020) Preparation and biomedical applications of multicolor carbon dots: recent advances and future challenges. Part Part Syst Charact 37(4):1900489
61. Tade RS et al (2020) Recent advancement in bio-precursor derived graphene quantum dots: synthesis, characterization and toxicological perspective. Nanotechnology 31(29):292001
62 Li F, Yang D, Xu H (2019) Non-metal-heteroatom-doped carbon dots: synthesis and properties. Chem-A Eur J 25(5):1165–1176
63. Shi, Y., et al 2021 *Carbon dots: an innovative luminescent nanomaterial.* Aggregate, e108.
64. Shen C-L et al (2020) Chemiluminescent carbon dots: synthesis, properties, and applications. Nano Today 35:100954
65. Sakdaronnarong C et al (2020) Recent developments in synthesis and photocatalytic applications of carbon dots. Catalysts 10(3):320
66. Jiang L et al (2020) UV–Vis–NIR full-range responsive carbon dots with large multiphoton absorption cross sections and deep-red fluorescence at nucleoli and in vivo. Small 16(19):2000680
67. Ding C, Zhu A, Tian Y (2014) Functional surface engineering of C-dots for fluorescent biosensing and in vivo bioimaging. Acc Chem Res 47(1):20–30
68. Yi, S., et al 2021 *Red emissive two-photon carbon dots: photodynamic therapy in combination with real-time dynamic monitoring for the nucleolus.* Carbon
69. Mintz KJ, Zhou Y, Leblanc RM (2019) Recent development of carbon quantum dots regarding their optical properties, photoluminescence mechanism, and core structure. Nanoscale 11(11):4634–4652
70. Xu Q et al (2019) Function-driven engineering of 1D carbon nanotubes and 0D carbon dots: mechanism, properties and applications. Nanoscale 11(4):1475–1504
71. Wang Y et al (2013) Luminescent carbon dots in a new magnesium aluminophosphate zeolite. Chem Commun 49(79):9006–9008
72. Basiri H et al (2020) Carbon dots conjugated with vascular endothelial growth factor for protein tracking in angiogenic therapy. Langmuir 36(11):2893–2900
73. Gavrilyuk S et al (2007) Many-photon dynamics of photobleaching. J Phys Chem A 111(47):11961–11975
74. Kozák OE et al (2013) Surfactant-derived amphiphilic carbon dots with tunable photoluminescence. J Phys Chem C 117(47):24991–24996
75. Sharma V et al (2018) Full color emitting fluorescent carbon material as reversible pH sensor with multicolor live cell imaging. J Photochem Photobiol, B 182:137–145
76. He H et al (2017) High-density super-resolution localization imaging with blinking carbon dots. Anal Chem 89(21):11831–11838
77. Gupta A, Nandi CK (2017) PC12 live cell ultrasensitive neurotransmitter signaling using high quantum yield sulphur doped carbon dots and its extracellular Ca^{2+} ion dependence. Sens Actuators, B Chem 245:137–145
78. Miao S, Liang K, Kong B (2020) Förster resonance energy transfer (FRET) paired carbon dot-based complex nanoprobes: versatile platforms for sensing and imaging applications. Mater Chem Front 4(1):128–139
79. Kumar A et al (2020) A design of fluorescence-based sensor for the detection of dopamine via FRET as well as live cell imaging. Microchemical Journal 159:105590
80. Kozma E, Kele P (2019) Fluorogenic probes for super-resolution microscopy. Org Biomol Chem 17(2):215–233
81. Hua X-W et al (2019) Nucleolus-targeted red emissive carbon dots with polarity-sensitive and excitation-independent fluorescence emission: high-resolution cell imaging and in vivo tracking. ACS Appl Mater Interfaces 11(36):32647–32658
82. Park SY et al (2017) Advanced carbon dots via plasma-induced surface functionalization for fluorescent and bio-medical applications. Nanoscale 9(26):9210–9217
83. Song Y et al (2017) Drug-derived bright and color-tunable N-doped carbon dots for cell imaging and sensitive detection of Fe^{3+} in living cells. ACS Appl Mater Interfaces 9(8):7399–7405
84. Gao G et al (2018) On-off-on fluorescent nanosensor for Fe^{3+} detection and cancer/normal cell differentiation via silicon-doped carbon quantum dots. Carbon 134:232–243
85. Esfandiari N et al (2019) Effect of carbonization degree of carbon dots on cytotoxicity and photo-induced toxicity to cells. Heliyon 5(12):e02940
86. Khajuria DK et al (2017) Fluorescent nanoparticles with tissue-dependent affinity for live zebrafish imaging. ACS Appl Mater Interfaces 9(22):18557–18565
87. Yang X-C et al (2020) One stone, two birds: pH-and temperature-sensitive nitrogen-doped carbon dots for multiple anti-counterfeiting and multiple cell imaging. ACS Appl Mater Interfaces 12(18):20849–20858
88. Cui Y et al (2015) Simple and efficient synthesis of strongly green fluorescent carbon dots with upconversion property for direct cell imaging. Part Part Syst Charact 32(5):542–546
89. Tadesse A et al (2020) Fluorescent-nitrogen-doped carbon quantum dots derived from citrus lemon juice: green synthesis, mercury (II) ion sensing, and live cell imaging. ACS Omega 5(8):3889–3898
90. Singh VK et al (2019) Nitrogen doped fluorescent carbon quantum dots for on-off-on detection of Hg^{2+} and glutathione in aqueous medium: live cell imaging and IMPLICATION logic gate operation. J Photochem Photobiol A: Chem 384:112042
91. Gu D et al (2018) Nitrogen and sulfur co-doped highly luminescent carbon dots for sensitive detection of Cd (II) ions and living cell imaging applications. J Photochem Photobiol, B 186:144–151
92. Kumari A et al (2018) Synthesis of green fluorescent carbon quantum dots using waste polyolefins residue for Cu^{2+} ion sensing and live cell imaging. Sensors and Actuators B: Chemical 254:197–205
93. Jana J et al (2016) One pot synthesis of intriguing fluorescent carbon dots for sensing and live cell imaging. Talanta 150:253–264

94. Fu C, Qian K, Fu A (2017) Arginine-modified carbon dots probe for live cell imaging and sensing by increasing cellular uptake efficiency. Mater Sci Eng, C 76:350–355
95. Francis L et al (2020) Utilising magnetically isolated lysosomes for direct quantification of intralysosomal drug concentrations by LC-MS/MS analysis: an investigatory study with imipramine. J Pharm Sci 109(9):2891–2901
96. Yu F et al (2016) The role of lysosome in cell death regulation. Tumor Biology 37(2):1427–1436
97. Mohammadi S et al (2021) An experimental investigation on the influence of various buffer concentrations, osmolytes and gold nanoparticles on lysozyme: spectroscopic and calorimetric study. Int J Biol Macromol 172:162–169
98. Ge W et al (2015) The roles of lysosomes in inflammation and autoimmune diseases. Int Rev Immunol 34(5):415–431
99. Zhao, Q., S.M. Gao, and M.C. Wang 2020 *Molecular mechanisms of lysosome and nucleus communication.* Trends in Biochemical Sciences
100. Fang M et al (2019) Fluorescent probe based on carbon dots/silica/molecularly imprinted polymer for lysozyme detection and cell imaging. Anal Bioanal Chem 411(22):5799–5807
101. Liu Q et al (2020) Carbon dots for lysosome targeting and imaging of lysosomal pH and Cys/Hcy in living cells. Nanoscale 12(24):13010–13016
102. Chen, X., X. Zhang, and F.-G. Wu 2021 *Ultrasmall green-emitting carbon nanodots with 80% photoluminescence quantum yield for lysosome imaging.* Chinese Chemical Letters
103. Qin H et al (2020) A wash-free lysosome targeting carbon dots for ultrafast imaging and monitoring cell apoptosis status. Anal Chim Acta 1106:207–215
104. Wang W-J et al (2016) Green preparation of carbon dots for intracellular pH sensing and multicolor live cell imaging. Journal of Materials Chemistry B 4(44):7130–7137
105. Chang S et al (2020) Label-free chlorine and nitrogen-doped fluorescent carbon dots for target imaging of lysosomes in living cells. Microchim Acta 187(8):1–8
106. Sun Y et al (2020) Rational design of far-red to near-infrared emitting carbon dots for ultrafast lysosomal polarity imaging. ACS Appl Mater Interfaces 12(28):31738–31744
107. Tong L et al (2020) One-step fabrication of functional carbon dots with 90% fluorescence quantum yield for long-term lysosome imaging. Anal Chem 92(9):6430–6436
108. Zhou D et al (2021) Lysosome-targetable selenium-doped carbon nanodots for in situ scavenging free radicals in living cells and mice. Microchim Acta 188(7):1–8
109. Wang, P., et al 2021 *One-pot synthesis of nuclear targeting carbon dots with high photoluminescence.* Chinese Chemical Letters
110. Havrdová M et al (2021) Self-targeting of carbon dots into the cell nucleus: diverse mechanisms of toxicity in NIH/3T3 and L929 cells. Int J Mol Sci 22(11):5608
111. Datta K et al (2014) Quaternized carbon dot-modified graphene oxide for selective cell labelling–controlled nucleus and cytoplasm imaging. Chem Commun 50(74):10782–10785
112. Lu S et al (2016) Hydrothermal synthesis of nitrogen-doped carbon dots with real-time live-cell imaging and blood–brain barrier penetration capabilities. Int J Nanomed 11:6325
113. Farley KI et al (2015) Determinants of mammalian nucleolar architecture. Chromosoma 124(3):323–331
114. Penzo M et al (2019) The ribosome biogenesis—cancer connection. Cells 8(1):55
115 Sen Gupta A, Sengupta K (2017) Lamin B2 modulates nucleolar morphology, dynamics, and function. Mole Cell Biol 37(24):e00274-17
116. Stimpson KM et al (2014) Nucleolar organization, ribosomal DNA array stability and acrocentric chromosome integrity are linked to telomere function. PLoS One 9(3):e92432
117. Lara-Martínez R et al (2016) Morphological studies of nucleologenesis in Giardia lamblia. Anat Rec 299(5):549–556
118. Cao C et al (2019) Ribosomal RNA-selective light-up fluorescent probe for rapidly imaging the nucleolus in live cells. ACS sensors 4(5):1409–1416
119. Feng R et al (2017) Turn-on fluorescent probes that can light up endogenous RNA in nucleoli and cytoplasm of living cells under a two-photon microscope. RSC Adv 7(27):16730–16736
120. Li H et al (2019) Biocompatible carbon dots with low-saturation-intensity and high-photobleaching-resistance for STED nanoscopy imaging of the nucleolus and tunneling nanotubes in living cells. Nano Res 12(12):3075–3084
121. Liu Y et al (2016) A cyanine dye to probe mitophagy: simultaneous detection of mitochondria and autolysosomes in live cells. J Am Chem Soc 138(38):12368–12374
122. Wallace DC (2005) A mitochondrial paradigm of metabolic and degenerative diseases, aging, and cancer: a dawn for evolutionary medicine. Annu Rev Genet 39:359–407
123. Gao G et al (2017) Mitochondria-targetable carbon quantum dots for differentiating cancerous cells from normal cells. Nanoscale 9(46):18368–18378
124. Zhao J et al (2020) A multifunctional nanoprobe for targeting tumors and mitochondria with singlet oxygen generation and monitoring mitochondrion pH changes in cancer cells by ratiometric fluorescence imaging. Chem Sci 11(14):3636–3643
125. Gong N et al (2019) Carbon-dot-supported atomically dispersed gold as a mitochondrial oxidative stress amplifier for cancer treatment. Nat Nanotechnol 14(4):379–387
126. Hua X-W et al (2017) Carbon quantum dots with intrinsic mitochondrial targeting ability for mitochondria-based theranostics. Nanoscale 9(30):10948–10960
127. Geng X et al (2019) Retrosynthesis of tunable fluorescent carbon dots for precise long-term mitochondrial tracking. Small 15(48):1901517
128. Guo S et al (2020) Fluorescent carbon dots shuttling between mitochondria and the nucleolus for in situ visualization of cell viability. ACS Appl Bio Mater 4(1):928–934
129. Almanza A et al (2019) Endoplasmic reticulum stress signalling—from basic mechanisms to clinical applications. FEBS J 286(2):241–278
130. Yoshida H (2007) ER stress and diseases. FEBS J 274(3):630–658
131. Shuang E et al (2021) Correction: Carbon dots with tunable dual emissions: from the mechanism to the specific imaging of endoplasmic reticulum polarity. Nanoscale 13(5):3307–3307
132. Ohsaki Y, Suzuki M, Fujimoto T (2014) Open questions in lipid droplet biology. Chem Biol 21(1):86–96
133. Onal G et al (2017) Lipid droplets in health and disease. Lipids Health Dis 16(1):1–15
134. Liu M-X et al (2021) One-step synthesis of carbon nanoparticles capable of long-term tracking lipid droplet for real-time monitoring of lipid catabolism and pharmacodynamic evaluation of lipid-lowering drugs. Anal Chem 93(12):5284–5290
135. Wang, J., et al 2021 *Quantitative structure–activity relationship enables the rational design of lipid droplet-targeting carbon dots for visualizing bisphenol A-induced nonalcoholic fatty liver disease-like changes.* ACS Applied Materials & Interfaces
136 Zhuang Q et al (2020) A self-adaptive multi-color fluorescent pH probe with the ability of whole cell imaging. Talanta 208:119780
137. Lesani, P., et al 2021 *Two-photon ratiometric carbon dot-based probe for real-time intracellular pH monitoring in 3D environment.* Chemical Engineering Journal 133668

138. Yang Z et al (2013) Fluorescent pH sensor constructed from a heteroatom-containing luminogen with tunable AIE and ICT characteristics. Chem Sci 4(9):3725–3730
139. Feng Y et al (2014) New fluorescent pH sensor based on label-free silicon nanodots. Sens Actuators, B Chem 203:795–801
140. Xiaoqing L et al (2015) Ultra sensitive and wide-range pH sensor based on the BSA-capped Cu nanoclusters fabricated by fast synthesis through the use of hydrogen peroxide additive. RSC Adv 5(60):48835–48841
141. Liu C et al (2021) A mini review on pH-sensitive photoluminescence in carbon nanodots. Front Chem 8:1242
142. Wang Q et al (2019) Strong acid-assisted preparation of green-emissive carbon dots for fluorometric imaging of pH variation in living cells. Microchim Acta 186(7):1–9
143. Wang N et al (2018) Deep eutectic solvent-assisted preparation of nitrogen/chloride-doped carbon dots for intracellular biological sensing and live cell imaging. ACS Appl Mater Interfaces 10(9):7901–7909
144. Shi B et al (2016) Nitrogen-rich functional groups carbon nanoparticles based fluorescent pH sensor with broad-range responding for environmental and live cells applications. Biosens Bioelectron 82:233–239
145. Ehtesabi H et al (2020) Carbon dots with pH-responsive fluorescence: a review on synthesis and cell biological applications. Microchim Acta 187(2):1–18
146. Bagheri Z et al (2015) Spectral properties and thermal stability of AS1411 G-quadruplex. Int J Biol Macromol 72:806–811
147. Rasekh B et al (2014) Protein engineering of laccase to enhance its activity and stability in the presence of organic solvents. Eng Life Sci 14(4):442–448
148. Kumar A et al (2017) Green synthesis of carbon dots from Ocimum sanctum for effective fluorescent sensing of Pb^{2+} ions and live cell imaging. Sens Actuators, B Chem 242:679–686
149. Yang S et al (2018) Anomalous enhancement of fluorescence of carbon dots through lanthanum doping and potential application in intracellular imaging of ferric ion. Nano Res 11(3):1369–1378
150. Singh AK et al (2019) One pot hydrothermal synthesis of fluorescent NP-carbon dots derived from Dunaliella salina biomass and its application in on-off sensing of Hg (II), Cr (VI) and live cell imaging. J Photochem Photobiol, A 376:63–72
151. Batool, M., et al 2020 *Metal ion detection by carbon dots—a review.* Critical Reviews in Analytical Chemistry, 1–12
152. Du F et al (2020) Facile synthesis of ultrahigh fluorescence N, S-self-doped carbon nanodots and their multiple applications for H 2 S sensing, bioimaging in live cells and zebrafish, and anti-counterfeiting. Nanoscale 12(39):20482–20490
153. Liang C et al (2021) Biomass carbon dots derived from Wedelia trilobata for the direct detection of glutathione and their imaging application in living cells. Journal of Materials Chemistry B 9(28):5670–5681
154. Pang L-F et al (2021) Cell membrane-targeted near-infrared carbon dots for imaging of hydrogen sulfide released through the cell membrane. Sensors and Actuators B: Chemical 345:130403
155. Ren G et al (2020) Efficient preparation of nitrogen-doped fluorescent carbon dots for highly sensitive detection of metronidazole and live cell imaging. Spectrochimica Acta Part A: Molecular and Biomolecular Spectroscopy 234:118251
156. Sun J et al (2019) 2, 4-Dinitrobenzenesulfonate-functionalized carbon dots as a turn-on fluorescent probe for imaging of biothiols in living cells. Microchim Acta 186(7):1–9
157. Deng Z et al (2020) A nanoprobe for ratiometric imaging of glutathione in living cells based on the use of a nanocomposite prepared from dual-emission carbon dots and manganese dioxide nanosheets. Microchim Acta 187(9):1–10
158. Wang, Q., et al 2021 *Nonblinking carbon dots for imaging and tracking receptors on a live cell membrane.* Chemical Communications
159. Wang, G.-G., et al 2021 *Carbon dots-based red fluorescence nanoprobe for caspase-1 activity assay and living cell imaging.* Sensors and Actuators B: Chemical 130285
160. Wang J et al (2015) High performance photoluminescent carbon dots for in vitro and in vivo bioimaging: effect of nitrogen doping ratios. Langmuir 31(29):8063–8073
161. Tang J et al (2013) Carbon nanodots featuring efficient FRET for real-time monitoring of drug delivery and two-photon imaging. Adv Mater 25(45):6569–6574
162. Ermis, E., et al 2021 *Red emissive NS co-doped carbon dots for live imaging of tumor spheroid in the microfluidic device.* Journal of Science: Advanced Materials and Devices
163. Hu J et al (2021) Spying on the polarity dynamics during wound healing of zebrafish by using rationally designed carbon dots. Adv Healthcare Mater 10(14):2002268
164. Rodrigues CV et al (2015) Down-and up-conversion photoluminescence of carbon-dots from brewing industry waste: application in live cell-imaging experiments. J Braz Chem Soc 26:2623–2628
165. Yu C et al (2013) Carbon-dot-based ratiometric fluorescent sensor for detecting hydrogen sulfide in aqueous media and inside live cells. Chem Commun 49(4):403–405